

A New Polymeric Binder for Silicon-Carbon Nanotube Composites in Lithium Ion Battery

Joonwon Bae^{*1}, Sang-Ho Cha², and Jongnam Park^{*3}

¹Department of Applied Chemistry, Dongduk Women's University, Seoul 136-714, Korea

²Department of Chemical Engineering, Kyonggi University, Gyeonggi 443-760, Korea

³Interdisciplinary School of Green Energy, Ulsan National Institute of Science and Technology (UNIST), Ulsan 689-798, Korea

Received August 9, 2012; Revised September 11, 2012; Accepted September 11, 2012

Abstract: We introduced polyethyleneimine (PEI) as a new binder for silicon (Si)-carbon nanotube (CNT) anode materials in lithium ion batteries (LIBs). The PEI binder was chosen to enhance the binding of electrode material containing Si-CNT nanocomposites through the formation of a PEI thin layer on the surfaces of CNTs. It was expected that the spontaneous electrostatic interactions between weakly charged PEI molecules with CNT surfaces could promote the binding performance. In other words, the formation of solid-electrolyte interface (SEI) could be suppressed owing to the effect of dominant electrostatic interactions between PEIs and CNTs. Zeta potential analyses demonstrated the real presence of electrostatic interactions between PEIs and CNTs. Accordingly, lithium battery half-cell tests showed that improved capacity retention behavior was observed in the sample with PEI than that with polyvinylidene fluoride (PVDF) binder. Remarkably, for the case of Si-CNT anode materials prepared without or with relatively less amount of CNT, a higher reduction in capacity was observed with PEI binder than with PVDF. An additional advantage of the incorporation of PEI binder is an increase of initial coulombic efficiency approximately 5%~10%. Consequently, all these findings support that PEI is highly desirable as an alternative binder for electrode materials containing CNT.

Keywords: silicon, carbon nanotubes, polyethyleneimine, binder, lithium ion battery, electrostatic interaction.

Introduction

There have been several issues in rechargeable battery technology, such as high energy density, high power, safety, and cost. Among them, the demand for high energy density materials is rapidly increasing to keep pace with the fast developing speed of high performance mobile devices. To date, a lot of researchers have invested efforts to develop electrode materials which retain those advantages. Silicon (Si) as an anode material in lithium ion battery (LIB) has been extensively studied due to its high specific capacity (4,200 mAh/g)¹⁻⁴ compared with that of graphite (372 mAh/g).⁵ However, Si or Si-based composite materials have not yet reached at a reliable state for commercialization. One of the reasons is the deterioration of capacity originated from the volume expansion (~400% for Li₂₂Si₅) and contraction upon Li insertion and extraction. Repeated volume change upon cycling causes the pulverization of active materials leading to the loss of electric conduction pathway and finally capacity fade.⁶⁻⁸ In addition, inherent low electrical conductivity

of Si tends to degrade overall battery performance due to high impedance of electron flow during electrochemical process. Therefore, numerous ideas have been suggested to minimize the volume change and to increase the electrical conductivity.^{9,10} Several remarkable approaches are the use of nanometer sized silicon¹¹ and preparation of composites with carbon materials such as amorphous carbon,^{12,13} aerogel,¹⁴ and carbon nanotubes.¹⁵⁻¹⁹

Among promising methods, the introduction of CNTs for composites formation with Si has been attractive owing to the excellent electrical conductivity, dimensional stability and flexibility, and chemical inertness of CNTs. However, Si-CNT composites have not yet been developed successfully because of some practical difficulties. One of the most critical issue is the high specific surface area of CNTs (100~1,000 m²/g depending on types), which results in a low initial coulombic efficiency through the formation of solid-electrolyte interface (SEI) on large surface of CNTs. Generally, an initial efficiency of higher than 85% in a half cell is accepted as a prerequisite for design of full cell batteries. The other issue is the uniform dispersion of CNTs in resultant composites. Several popular processes for composite preparation are direct growth of CNTs, use of surfactants, and ball

*Corresponding Authors. E-mails: joonwonbae@gmail.com or jnpark@unist.ac.kr

and roll milling methods. In the previous work, it was revealed that a wet-type milling is a powerful tool for CNT dispersion in silicon, where even a small amount of CNTs can effectively network the simultaneously pulverized silicon nanograins.²⁰ But, a substantially stronger linkage such as a covalent bond between them is necessary not only for an efficient electrical conduction in the composites but also for the maintenance of structural durability under a severe mechanical stress by an excessive volume change. So a calcination process was employed to attain a stronger bond formation. Based on these facts, we reported the successful preparation and application of Si-CNT nanocomposites as anode, and characteristics of Li charge/discharge behavior.²⁰

On the other hand, strong cohesion between active species in electrode materials is also important to keep the electrical conduction path during Li insertion and extraction processes. One plausible approach to circumvent the large formation of SEI is the surface modification of CNTs in order to prevent the electrochemical reduction of electrolyte on CNT surface. If the resistive layer has a capability to bind electrode materials, the problem of low initial efficiency arising from CNTs' high surface area could be solved. Surface functionalization of graphite by polymer coating was tried to decrease irreversible capacity.²¹ Therefore, a new binder system for Si-CNT composite has been introduced to improve the binding performance between Si and CNT. Occasionally, carboxymethyl cellulose (CMC) binder was reported to show excellent performance in capacity retention for Si based anode materials compared with polyvinylidene fluoride (PVDF) binder.²²⁻²⁶ The main function of CMC is the maintenance of crosslinked structure through chemical bond formation between hydroxyl group of Si surface and carboxylic group of CMC binder. That is, a pursuit for better binder might motivate researchers for a faster realization of batteries with high energy density.

As a context of consistent research, the application of a new binder, polyethyleneimine (PEI) for Si-CNT nanocomposite is studied in this article. PEI was selected to enhance the binding of electrode material through the potential electrostatic interaction of weakly charged PEI molecules with CNTs. It is known that electron donating groups such as imine in PEI interact spontaneously with sidewalls of CNTs *via* charge-transferred physisorption.²⁷⁻²⁹ The effectiveness of PEI was compared with that of PVDF as a function of CNT composition in composites.

Experimental

Materials. Silicon nanoparticle with an average diameter of 4 μm was purchased from High Purity Chemical Co. (Japan). Single walled carbon nanotube was purchased from Carbon Nanotechnologies Inc. (USA). A binder polyethyleneimine (PEI) and polyvinylidene fluoride (PVDF) were purchased from Sigma-Aldrich (Wisconsin, US). All solvents were used as

received without further purification.

Preparation of Si-CNT Nanocomposites. Si-CNT nanocomposites were prepared by a wet type beads milling method. The mixture of Si nanopowder and CNT in a weight of 9:1 was crushed in an alcoholic liquid such as ethanol or octanol by beadsmill treatment (Ultra Apex Mill UAM-015, Kotobuki Ind. Co. Ltd., Japan). Fine slurry was obtained in the condition of 55 Hz for one or two hours using 0.1 mm sized zircornia beads. Then, Si-CNT nanocomposite was obtained by drying at 120 °C in air convection oven overnight.

Electrode Preparation and Half Cell Test. Si-CNT nanocomposites (55 wt%) and graphite (SFG-6, Timcal, Switzerland) used as a conducting additive (30 wt%) were mixed in a mortar, then a binder (PEI, 15 wt%) or polyvinylidene fluoride (PVDF, 15 wt%) was added and agitated. The solvents for PEI and PVDF were deionized water and *N*-methylpyrrolidone (NMP), respectively. For the case of electrode without graphite, Si-CNT nanocomposite (80 wt%) were mixed with binder (20 wt%). Then each paste was coated onto a 15 μm -thick copper foil and dried at 120 °C in a vacuum oven for 2 h. For half cell test, the electrode was pressed and punched in 12 mm diameter circle, then assembled in a coin-type cell (CR2016) with lithium metal counter electrode, polytetrafluoroethylene (PTFE) separator, and electrolyte (1.3 M LiPF₆ in EC/DEC 3:7 volume ratio, Cheil Industries Inc., Korea). Electrochemical measurements were performed at a rate of 0.2 C in a voltage range of 0~1.5 V vs. Li/Li⁺.

Characterizations. The morphology of Si-CNT nanocomposite was observed using a JEOL 6700 field emission scanning electron microscope (FE-SEM). The nitrogen adsorption-desorption isotherms and surface areas were obtained with a Micromeritics ASAP 2000 instrument at 77 K. X-Ray diffraction patterns were recorded on a Rigaku Geigerflex diffractometer. Nuclear magnetic resonance spectra were recorded on a Bruker AVANCE III (600 MHz) spectrometer. Zeta potential was measured with a ESA9800 Zeta potential Analyzer (Matec Applied Science) with a standard 633 nm laser in water solvents.

Results and Discussion

Figure 1 shows the SEM images of Si-CNT nanocomposite prepared by a wet-milling method. Figure 1(a) indicates that the dominant shape of Si particles is thin sub-micron platelet with average thickness of tens of nanometer while CNTs are dispersed homogeneously in the nanocomposite. The significant shear forces induced by the random movements of zircornia beads lead to the unavoidable breakage of Si powders. At the same time, mixing of resulting Si nanoparticles with CNTs could also be promoted with the aid of same driving force. A closer look at the Si-CNT nanocomposite in Figure 1(b) shows the absence of remarkable aggregations of CNTs. This fact is critical for the performance retention

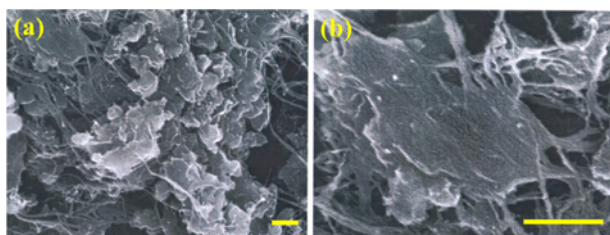


Figure 1. SEM images of Si-CNT nanocomposites prepared with a wet-type milling method taken at relatively (a) low and (b) high magnifications. Scale bar 200 nm.

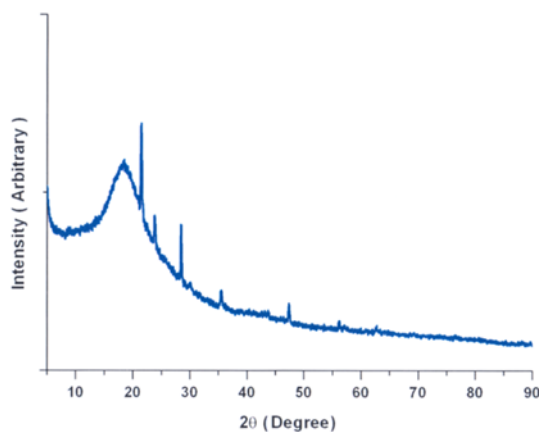


Figure 2. Typical XRD diffraction pattern of Si-CNT nanocomposites prepared with a wet beadsmilling method.

of the final nanocomposite as anode in LIBs because the local aggregations of CNTs inside nanocomposites cause deterioration in initial efficiency, capacity, and lifetime. In a word, it was revealed that the milling process using 0.1 mm zirconia beads in a liquid medium achieved the crushing of silicon powder into nanoparticles and the effective dispersion of CNTs, simultaneously. The randomly distributed voids can accommodate the volume expansion/shrinkage during charge/discharge processes.

The formation of Si-CNT was further confirmed by X-ray diffraction as shown in Figure 2. The appearances of characteristic diffraction peaks demonstrated the successful preparation of nanocomposites. In order to obtain quantitative data, Scherrer equation was introduced. The Scherrer equation relates the width of a power diffraction peak to the average (by volume) dimensions of crystallites in a polycrystalline powder.

$$\beta_s(2\theta)_{hkl} = \frac{K\lambda}{T\cos\theta_{hkl}}$$

where β_s is the crystallite size contribution to the peak width (integral of full width at half maximum) in radians, K is constant near unity, and T is the average thickness of the crystal in a direction normal to the diffracting plane hkl . In interpreting the Scherrer equation, it is important not to con-

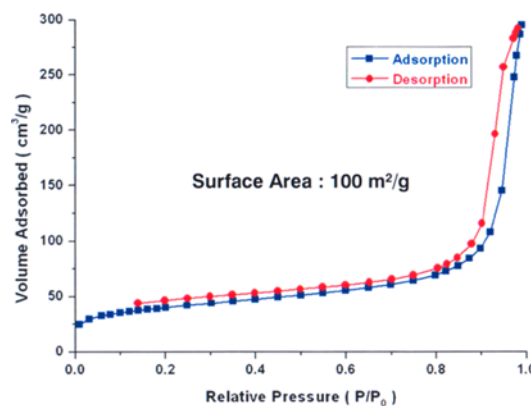


Figure 3. Nitrogen adsorption/desorption isotherms at 77 K of Si-CNT nanocomposites prepared with a wet beadsmilling method.

fuse the crystallite size with the size of the polycrystalline aggregate. In general, a “crystal” or “crystallite” refers to a discrete diffracting domain that coherently scatters X-rays.³⁰ Based on these facts, the average size range of silicon crystals/crystallites obtained by this equation was in the range of 14 to 30 nm depending on the liquid medium. Specifically, use of ethanol produces smaller silicon particles than n-octanol under the same milling condition (data not shown). As we can see with SEM images in Figure 1, this size range corresponds to the thickness of Si platelet. Compared with the original size of Si powder (4 μm), the effective mixing of wet type milling process was clearly demonstrated.

Before taking a look at electrochemical behavior, it is worthwhile to obtain specific surface area of Si-CNT nanocomposite with a nitrogen adsorption/desorption isotherms at 77 K. In general, high surface is undesirable for the prevention of SEI formation. The typical surface area of Si-CNT nanocomposite was approximately 100 m^2/g as revealed in Figure 3. This value is consistent with the typical surface area of commercial CNTs. The pore size distribution is unimportant in this case because there are only micropores on the surfaces of both Si nanoparticles and CNTs. Because the size of Si particles looked much larger than CNTs as seen in Figure 1, it is clear that CNTs contributed dominantly to the surface area. Therefore, the introduction of polymeric binder for the control of surface property of CNTs is a challenging and meaningful research task.

Figure 4 presents the solid state nuclear magnetic resonance spectra of pristine CNT and PEI/CNT mixture. Zeta potential values indicated on each spectrum are -8 and 19 mV, respectively. The characteristic peaks in the two NMR spectra are exactly identical. This fact supports that there are no structural changes for both PEI and CNTs.

But it is important to reveal the surface interaction between PEI and CNT. For zeta potential measurement, water was used as solvent. Thus, it is natural that there might be some solvent effect. However, the surface polyelectrolyte layer (such as poly(diallyl dimethyl ammonium chloride), poly

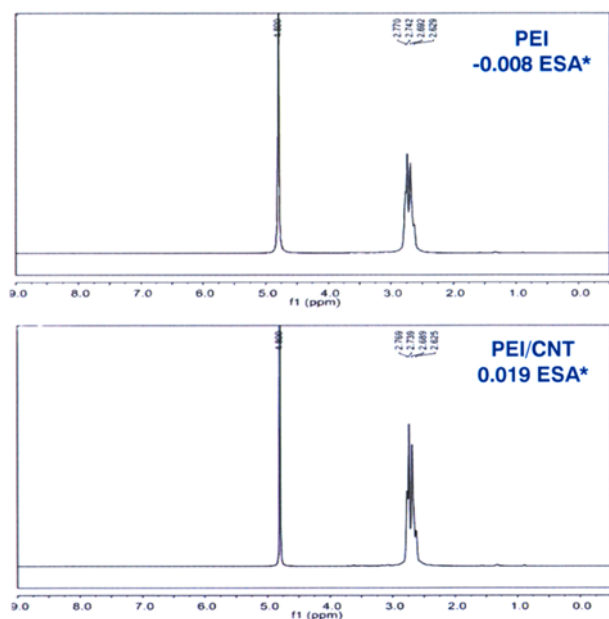


Figure 4. Solid state NMR spectra and zeta potentials of (a) pristine CNT and (b) PEI/CNT.

(ethyleneimine), poly(styrenesulfonate)) is known to remain intact after washing with water several times because the substantial surface interaction between polyelectrolyte and substrate is electrostatic.^{31,32}

On the other hand, in this experiment, we tried to reveal only the possibility for the modification of surface interaction by introduction of PEI binder. In general, the surface is considered to be neutral if zeta potential falls in the range of $-10 \sim +10$ mV. A surface is highly cationic or anionic if zeta potential is higher than $+10$ mV or lower than -10 mV, respectively. By measuring zeta potentials of CNT and CNT/PEI, we could see if the surface interaction is modified by the introduction of PEI binder. Judging from the significant zeta potential value change, it is clear that the surface properties can be modified by the introduction of PEI. That is, the possible interaction between PEI molecules and CNTs are one of those specific interactions accompanying no structural changes such as weak electrostatic interaction between partially induced electric charges, and hydrogen bonding. These interactions are spontaneous and stable under conventional experimental conditions employed in this work. It can also be inferred that the strong interaction is not influenced by the introduction of additional salt during lithium battery test. Therefore, it is inferred that the charged character of PEI can provide a potential effect on the performance as binder for LIB electrode. Based on these preliminary reasoning, the effect of PEI binder on electrochemical process is discussed in the following sections.

Figure 5 describes how PEI binder affects the electrochemical behavior of lithium half cell under conventional

testing conditions. When the PEI binder is mixed with prepared Si-CNT composites, the side branches of PEI molecules tend to wrap the surface of CNTs through the electrostatic interaction between amine derivative groups in PEI molecules and the weakly charged CNT surfaces. If this interaction is sufficiently strong to sustain the cohesion of electrode material during charge/discharge process, PEI can be considered as an applicable binder. An important requirement for reliable cycle life performance is maintaining the electrical conducting pathways between active materials in electrode during charge/discharge process. As addressed in previous paragraphs, PVDF binder for graphite and functionalized cellulose for Si based anodes can effectively keep the active electrode materials cohered. By analogy, PEI in Si-CNT nanocomposites can be expected to play a synergistic role to keep the active electrode materials as effective charge carriers in LIBs. Before the practical application of PEI as a binder, the electrochemical activity of pristine PEI was measured using the same charge/discharge conditions. An obtained capacity of the pristine PEI tested with lithium counter electrode was negligibly small (2 mAh/g).

The effectiveness of PEI binder was compared to the electrode prepared with conventional PVDF binder. Figure 5 exhibits the cyclic performances of Si-CNT nanocomposite electrodes made without graphite (a, b) and with graphite (c, d). Regardless of the addition of graphite conducting medium to the Si-CNT nanocomposites, PEI binder demonstrates a better cyclic performances than PVDF binder. A slight increase in the initial coulombic efficiency is associated with the addition of graphite with inherently high electrical conductivity. To verify the presence of possible interaction between PEI binder molecules and CNT surfaces, an additional experiment has been done using pure Si nanoparticle electrode (data not shown). This electrode was composed of Si nanoparticles and graphite, in which the Si nanoparticles were produced by the same wet-milling processing conditions as used for Si-CNT nanocomposite. When the CNTs were not combined with Si particles, fast degradation in capacity was observed whatever binder was used for electrode preparations. This might be attributed to the aggregation of Si nanoparticles without CNT networks, where electrical conducting pathways dramatically decreased thus a buffering space for volume change was not sufficiently ensured.

On the other hand, thermal annealing of Si-CNT nanocomposites almost dismissed the effect of different binder PEI and PVDF. Figure 6 displays the cyclic performance of Si-CNT with PEI and PVDF thermally treated for 2 h at 800°C under nitrogen atmosphere. Both PVDF and PEI exhibited conspicuously good cyclic performance keeping high capacities. Microscopically, PVDF shows a slightly better result but this fact delivers insignificant meaning. In general, polymer binders are very susceptible to the thermal annealing and thus a fair amount of polymer binder naturally degrades by the thermal treatment. Accordingly, surface interactions between

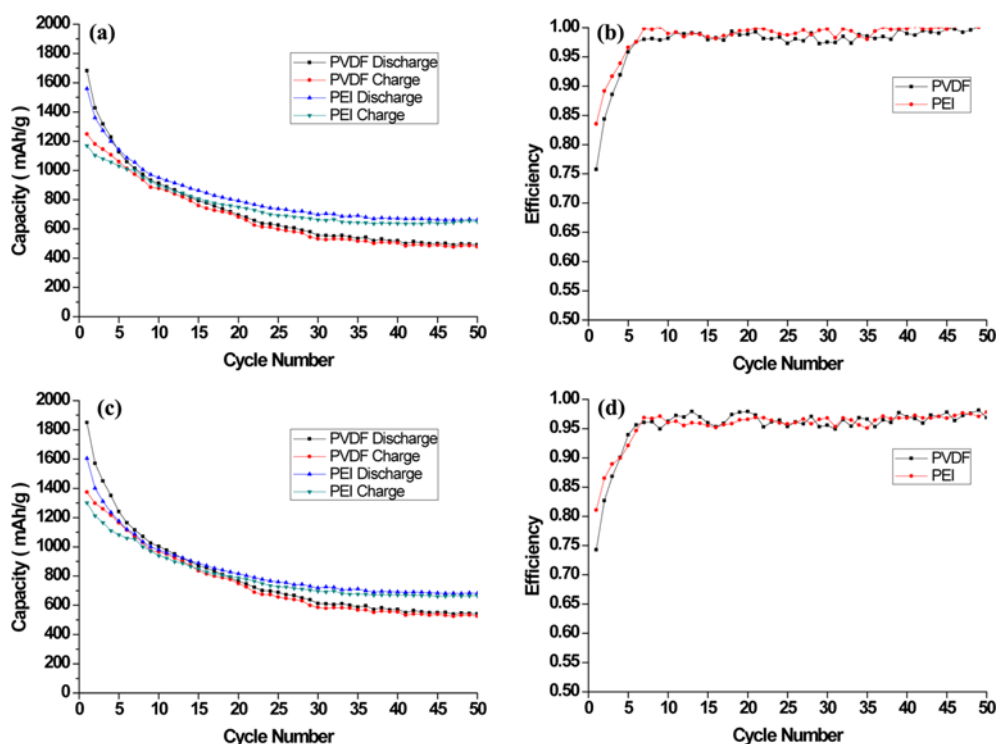


Figure 5. Cyclic performances of two different binders, PEI and PVDF, in charge/discharge capacities and coulombic efficiencies. (a), (b) Si-CNT and (c), (d) Si-CNT with graphite additive.

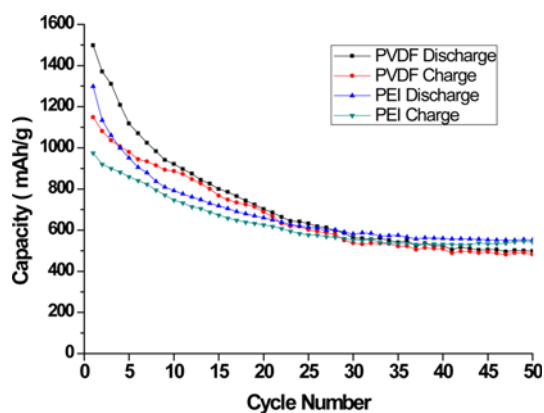


Figure 6. Cyclic performances of two different binders, PEI and PVDF, in charge/discharge capacities for Si-CNT thermally annealed at 800 °C for 2 h.

binder and other components should be relatively weaker. Therefore, those interactions such as Si-binder and CNT-binder would be less dominant after thermal annealing. Consequently, the cyclic performance of electrode is mainly determined by the performance of pristine Si and CNT. This experiment is also an indirect evidence for the presence of interactions between binder and other components.

In previous sections, we emphasize an approach to modify the surface of CNTs with a new binder interlayer acting as an electrical potential barrier to minimize the irreversible electrochemical reaction leading to SEI formation. In order

to validate the effect of PEI on CNT containing composites, the formation of SEI layer for each binder case was identified with differential capacity profiles. In the inset of Figure 7(a) (same sample as for Figure 5(a)), the peak of the PVDF sample at 0.6 V vs. Li/Li⁺ in the first cycle is assigned to the formation of SEI, whereas the peak of the PEI sample is located at 0.45 V and relatively weak. This observation could be understood as the prevention of SEI formation on the PEI coated CNTs. On the other side, the first cycle in the inset of Figure 7(b) (same sample as for Figure 6) presents a similar peak height for SEI formation except -0.1 V shift in the PEI case. This fact indicates that the effect of PEI preventing the formation of SEI is insignificant for the thermally annealed Si-CNT nanocomposites.

In addition, the peaks of shoulders at lower voltages than the SEI formation on the first cycle for each sample, *i.e.* 0.3 V (PEI), 0.4 V (PVDF) in the inset of Figure 7(a) and 0.25 V (PEI), 0.32 V (PVDF) in the inset of Figure 7(b), are assigned to the decomposition of SiO_x to Si and Li₂O.³³ For both of Figure 7(a) and (b), the sharp and strong peaks at 0.07 V vs. Li/Li⁺ in the first cycle are associated with the conversion of crystalline Si to amorphous state of Li_xSi alloy.¹⁹ Once the amorphous state is created, the peaks of lithiation process appear in the broad range of 0.05 to 0.35 V vs. Li/Li⁺ from the second cycle. The differential capacities of the 10th cycle in Figure 7(b) represent almost same profiles for both binders, indicating no specific effect of PEI with respect to PVDF in the heat-treated Si-CNT nanocomposite due to loss of poly-

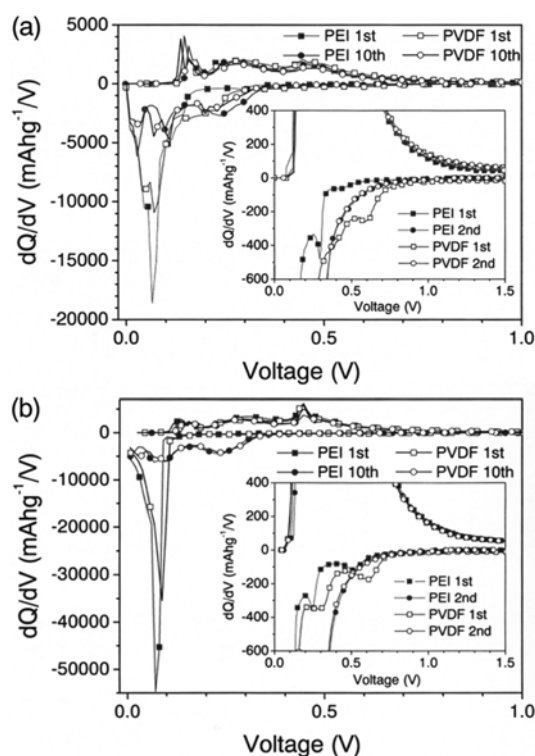


Figure 7. Differential capacity plots for two different binders, PEI and PVDF. Comparison of the 1st and 10th cycles of (a) Si-CNT (same sample as for Figure 5(a)) and (b) Si-CNT thermally treated at 800 °C for 2 h (same sample as for Figure 6). Insets are the comparison of the 1st and 2nd cycle plots of each sample.

meric binder and CNTs. This result is consistent with the reasoning addressed for the explanation of Figure 6.

Conclusions

An outstanding advantage of PEI binder for Si-CNT nanocomposite can be substantiated. The binding effect maintaining the cohesion of electrode material improves electrochemical cycle life performance, while the coating effect of PEI over CNTs increases initial and overall coulombic efficiencies. The negative effect of CNTs for electrode arising from high surface area could be avoided effectively by the use of PEI binder. The positive results presented in this study may stimulate further investigation of Si-CNT anode and binder system for practical commercialization.

References

- (1) R. A. Sharma and R. N. Seefurth, *J. Electrochem. Soc.*, **123**, 1763 (1976).
- (2) C. J. Wen and R. A. Huggins, *J. Solid State Chem.*, **37**, 271 (1981).
- (3) D. Fauteux and R. Koksang, *J. Appl. Electrochem.*, **23**, 1 (1993).
- (4) S. Bourderau, T. Brousse, and D. M. Schrich, *J. Power Sources*, **81-82**, 233 (1999).

- (5) S. Megahead and B. Scrosati, *J. Power Sources*, **51**, 79 (1994).
- (6) J. O. Besenhard, M. Hess, and P. Komenda, *Solid State Ionics*, **40-41**, 525 (1990).
- (7) M. Winter and J. O. Besenhard, *Electrochim. Acta*, **45**, 31 (1999).
- (8) L. F. Nazar and O. Crosnier, in *Lithium Batteries Sciences and Technology*, G.-A. Nazri and G. Pistoria, Eds., Kluwer Academic/Plenum, Boston, 2004, p 112.
- (9) J. H. Ryu, J. W. Kim, Y.-E. Sung, and S. M. Oh, *Electrochem. Solid-State Lett.*, **7**, A306 (2004).
- (10) S. Park, T. Kim, and S. M. Oh, *Electrochem. Solid-State Lett.*, **10**, A142 (2007).
- (11) C. K. Chan, H. Peng, G. Liu, K. McIlwath, X. F. Zhang, R. A. Huggins, and Y. Cui, *Nat. Nanotechnol.*, **3**, 31 (2008).
- (12) N. Dimov, S. Kugino, and M. Yoshio, *Electrochim. Acta*, **48**, 1579 (2003).
- (13) S. H. Ng, J. Wang, D. Wexler, S. Y. Chew, and H. K. Liu, *J. Phys. Chem. C*, **111**, 11131 (2007).
- (14) T. Hasegawa, S. R. Mukai, Y. Shirota, and H. Tamon, *Carbon*, **42**, 2573 (2004).
- (15) J. Y. Eom, J. W. Park, H. S. Kwon, and S. Rajendran, *J. Electrochem. Soc.*, **153**, A1678 (2006).
- (16) Z. S. Wen, J. Yang, B. F. Wang, K. Wang, and Y. Lui, *Electrochem. Commun.*, **8**, 51 (2006).
- (17) T. Kim, Y. H. Mo, K. S. Nahm, and S. M. Oh, *J. Power Sources*, **162**, 1275 (2006).
- (18) Y. Zhang, X. G. Zhang, H. L. Zhang, Z. G. Zhao, F. Li, C. Liu, and H. M. Cheng, *Electrochim. Acta*, **51**, 4994 (2006).
- (19) W. Wang and P. N. Kumta, *J. Power Sources*, **172**, 650 (2007).
- (20) J. Lee, J. Bae *et al.*, *J. Electrochem. Soc.*, **156**, A905 (2009).
- (21) H. Buqa, M. Holzapfel, F. Krumeich, C. Veit, and P. Novak, *J. Power Sources*, **161**, 617 (2006).
- (22) J. Li, R. B. Lewis, and J. R. Dahn, *Electrochem. Solid-State Lett.*, **10**, A17 (2007).
- (23) N. S. Hochgatterer, M. R. Schweiger, S. Koller, P. R. Raimann, T. Wöhrle, C. Wurm, and M. Winner, *Electrochem. Solid-State Lett.*, **11**, A76 (2008).
- (24) S. D. Beattie, D. Larcher, M. Morcrette, B. Simon, and J.-M. Tarascon, *J. Electrochem. Soc.*, **155**, A158 (2008).
- (25) J. L. Gómez Cámer, J. Morales, and L. Sánchez, *Electrochem. Solid-State Lett.*, **11**, A101 (2008).
- (26) J. Kong, N. R. Franklin, C. Zhou, M. G. Chapline, S. Peng, K. Cho, and H. Dai, *Science*, **287**, 622 (2000).
- (27) A. Star, J. P. Gabriel, K. Bradley, and G. Gruner, *Nano Lett.*, **3**, 459 (2003).
- (28) E. Muñoz, D.-S. Suh, S. Collins, M. Selvidge, A. B. Dalton, B. G. Kim, J. M. Razal, G. Ussery, A. G. Rinzier, M. T. Martínez, and R. H. Baughman, *Adv. Mater.*, **17**, 1064 (2005).
- (29) L. J. Fu, H. Liu, C. Li, Y. P. Wu, E. Rahm, R. Holze, and H. Q. Wu, *Solid State Sci.*, **8**, 113 (2006).
- (30) P. Scherrer and N. G. W. Gottingen, *Math-Phys. KI.*, **2**, 96 (1918).
- (31) M. Shen, S. H. Wang, X. Shi, X. Chen, Q. Huang, E. J. Petersen, R. A. Pinto, J. R. Baker Jr., and W. J. Weber Jr., *J. Phys. Chem. C*, **113**, 3150 (2009).
- (32) D. Q. Yang, J. F. Rochette, and E. Sacher, *J. Phys. Chem. B*, **109**, 4481 (2005).
- (33) H. Kim and J. Cho, *Nano Lett.*, **8**, 3688 (2008).